Mixed Ionic and Electronic Conduction in Radical Polymers

Ilhwan Yu, Daeyoung Jeon, Bryan Boudouris, and Yongho Joo*

Read Online

ACCESS | Metrics & More | Article Recommendations | Supporting Information

ABSTRACT: Organic mixed ionic and electronic conductors typically have heterogeneous conjugated macromolecular backbones and ether-based pendant groups to transport ions and charges. Moving from this archetype toward one with a single component, nonconjugated redox-active radical polymers that conduct both the charge and mass have significant benefits, such as they can be readily synthesized in large quantities and have the ability to produce either hole- or electron-transporting radical polymers by the selective tuning of the pedant group chemistry. Here, we demonstrate long-range (i.e., for lengths >50 μm) operational mixed ionic and electronic conduction in an amorphous, nonconjugated, low-glass-transition-temperature organic radical polymer upon blending the macromolecule with an ionic dopant lithium bis(trifluoromethanesulfonyl)imide salt (LiTFSI). Tuning the precise chemical nature of the functional radical pedant group using this ionic dopant is of key importance for the enhancement of long-range electrical conductivity. Moreover, the maximum ionic conductivity was 10^{-3} S cm^{-1} at elevated temperatures, and this was the highest reported value for a radical polymer-based system. Our findings demonstrate a significantly different macromolecular design paradigm than the commonly accepted heterogeneous composition for the creation of next-generation organic mixed ionic and electronic conductors.
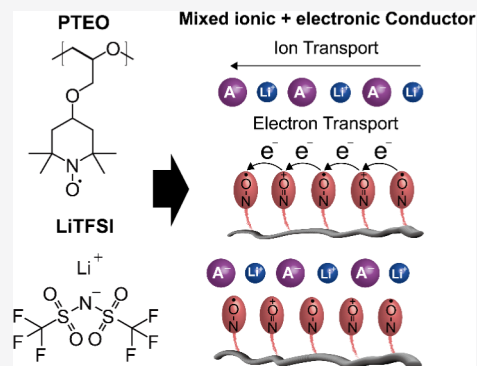

INTRODUCTION

Recently, radical polymers, defined as macromolecules composed of aliphatic carbon backbones and pedant stable radical groups, have garnered significant attention as active materials for high-performance transparent conductors,[1−3] fast-charging batteries,[4−7] high-efficiency solar cells,[8] light-emitting devices,[9,10] and other energy-related modules.[11−17] In these redox-active nonconjugated radical polymers, electron charge transfer occurs through electron hopping, and this is facilitated by the motion of the redox-active pedant groups.[7,18−21] Because of this process, charges are transported through the bulk of radical polymers by redox self-exchange reactions, and they can transfer charge across interfaces (e.g., at current-collecting electrodes) through heterogeneous redox reactions as well. These heterogeneous reactions, depending on the chemistry of the radical group, can be preferential to either oxidation or reduction from the neutral radical state. Thus, organic radicals can transport either holes (i.e., be p-type) or electrons (i.e., n-type) through the judicious selection of the pendant group chemistry. Hence, this handle provides various synthetic design routes for customization in myriad organic electronic applications.[22−25] One heavily evaluated application of radical polymers is their utilization in energy storage devices. For instance, the current champion organic radical polymer-based battery results in superfast charging−discharging rates (as high as 60C within 1 min)[7,23,26] and exceptional cyclability (i.e., >1000 cycles).[27,28]

In fact, these types of charge-transfer reactions have allowed nonconjugated radical polymers [i.e., poly(4-glycidyloxy-2,2,6,6-tetramethylpiperidine-1-oxyl) (PTEO) and poly-(2,2,6,6-tetramethylpiperidinyloxy methacrylate) (PTMA)] to exhibit solid-state electrical conductivity values of 10^{-5} S cm^{-1} for PTMA[29,30] and 0.2 S cm^{-1} for PTEO.[1] Higher electrical conductivity was observed in PTEO because a flexible macromolecular backbone and side-chain linker were part of the design motif.[1,31] The formation of a percolating network between electrodes upon thermal annealing above the glass transition temperature of PTEO leads to the high conductivity.[1] The reported value of electrical conductivity from PTEO is higher than those of several undoped conjugated polymers [e.g., poly(3-hexylthiophene) (P3HT) has an electrical conductivity of ∼10^{-6} S cm^{-1}].[32] Specifically, this charge transport through the radical polymer is possible due to the formation of a solid-state percolation structure of radical pendant groups that are in electronic communication. Importantly, this formation occurs despite the fact that the materials do not contain conjugated segments. However, this large electrical conductivity value was only obtained over
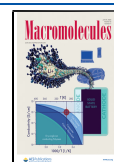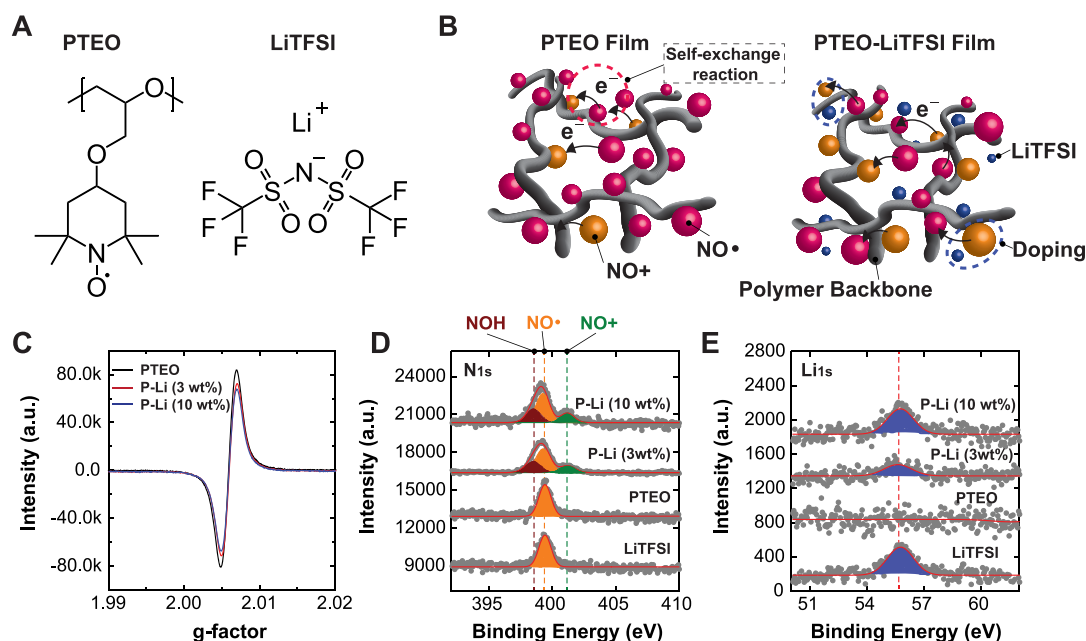
Figure 1. (A) Chemical structures of PTEO and LiTFSI. (B) Schematic illustration of the electron self-exchange reactions that occur for charge transport in radical polymers and the ionic doping that occurs as well. (C) EPR spectra of a radical polymer solution indicating that the radical content is relatively constant as a function of lithium salt doping. High-magnification X-ray photoelectron spectroscopy (XPS) spectra of PTEO thin films for (D) N_{1s} peaks and (E) Li_{1S} peaks. The PTEO radical polymer is oxidized with the addition of LiTFSI. Prior to film casting, the PTEO macromolecules were mixed with LiTFSI at concentrations of 3 and 10% (by weight). The spectra indicate three specific nitrogen chemical units (N−O$^\bullet$, $^+$N═O, and N−OH). The red line is associated with curve fits attributed to each peak from the gray dots (raw data). The cation peaks (green) enhance with increasing oxidation by LiTFSI.

relatively small channel lengths as the local order of radical groups could only be sustained over ∼600 nm in space. For larger channel dimensions, the solid-state electrical conductivity of the organic radical polymer was akin to an insulator ($\sim10^{-11}$ S cm^{-1}) for channel lengths >1 μm. To overcome this issue, we hypothesized that the introduction of ionic dopants would allow for strategic ionic−electronic coupling that could trigger electronic structural changes and subsequently regulate the electronic conductivity in these materials.

Until recently, only a few electronic and ionic efforts have been completed using macromolecules capable of serving as mixed conductors, and all of these studies focus on conjugated macromolecules.[33−36] That is, elucidating the fundamental aspects of mixed conduction in nonconjugated organic radical polymers has not been performed. In this work, we establish the charge conduction mechanism of radical polymers when they are mixed with ions in solid-state electronic devices, and these fundamental principles allow us to demonstrate the operation of these systems with device channel sizes in the micrometer length scale. First, we evaluated the effects of salt addition on the redox state of the functional pendant group. That is, because charge transport in the amorphous radical polymer is realized through the pedant radical groups, tuning the specific chemical nature of pedant functional groups is crucial. Moreover, as the redox self-exchange reaction in PTEO is promoted by the motion of the pedant group, the relaxation modes above T_g of the polymer chain have a great effect on charge transport, and we evaluate how the addition of ions to the film impacted the thermal properties of PTEO. That is, the addition of salt to the PTEO matrix affects the chain dynamics of the polymer and chemical nature of the radical pedant group, and this coupled impact causes an enhancement of the electrical conductivity of PTEO across long channel lengths.

Thus, we verified the complementary effects of ions and the radical polymer as the ionic, ionic−electronic, and electronic conductivity have been determined separately with a previously reported method.[33,37] These results highlight that doping the radical moiety in polymers positively impacts their ability to transport charges in the solid state and also shows that the physical property of polymer can affect the ionic transport, thus providing the design strategies for the functional macromolecules. As such, this effort introduces a means by which to transform the generally considered archetype with respect to molecular engineering of mixed ionic and electronic conductors by leveraging the self-exchange reaction kinetics and chemical doping linked to open-shell species and demonstrates a next-generation material direction in the realm of organic radical electronic devices and batteries.

■ RESULTS AND DISCUSSION

The radical polymer utilized in this effort, PTEO, consists of stable radical groups (2,2,6,6-tetramethyl piperidinyl N-oxyl, TEMPO) linked to a poly(ethylene oxide) backbone (Figure 1A).[31] Upon the oxidation of the neutral TEMPO radical, the pendant groups can transfer charge, resulting in an oxoammonium cation (Figure S1). A rapid electron self-exchange reaction occurs through the radical pendant group when the radical sites are in close proximity (Figure 1B).[25,27] For this type of charge transport, the radical density is critical to control, and the number of repeat units (i.e., the molecular weight of the PTEO) needs to be optimized for the aspired device performance throughout the operation. This is because the molecular weight of the polymer is closely related to its chain dynamics for one radical unit to communicate with another active radical unit so that the redox reaction occurs. As such, we polymerized a monomer following a previous report,[1]
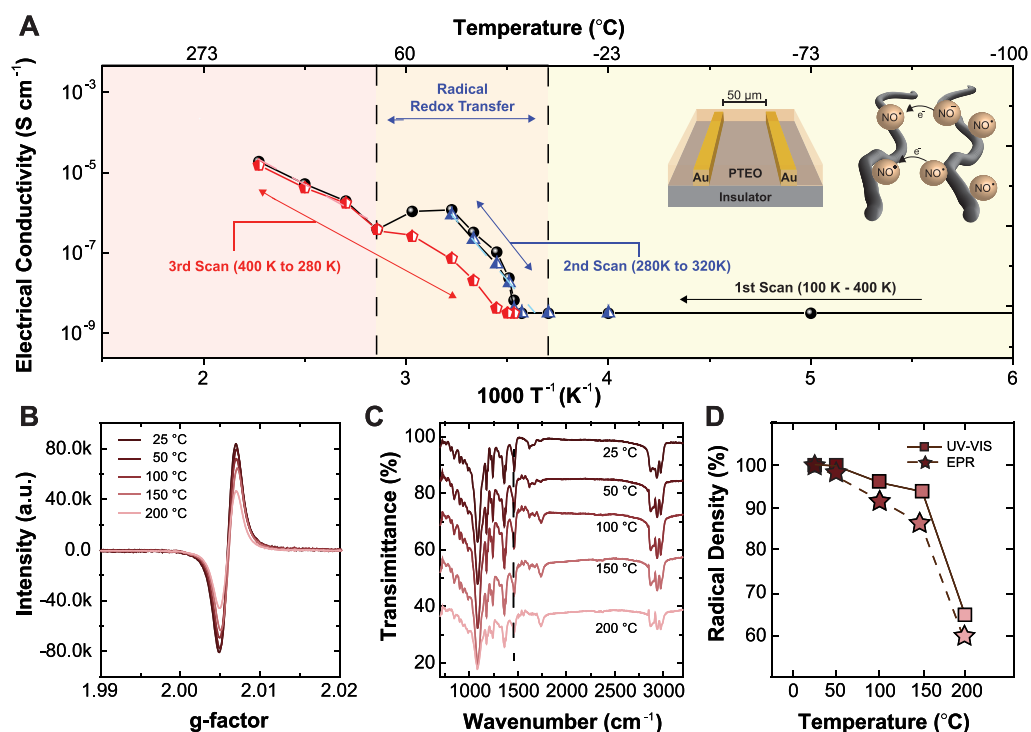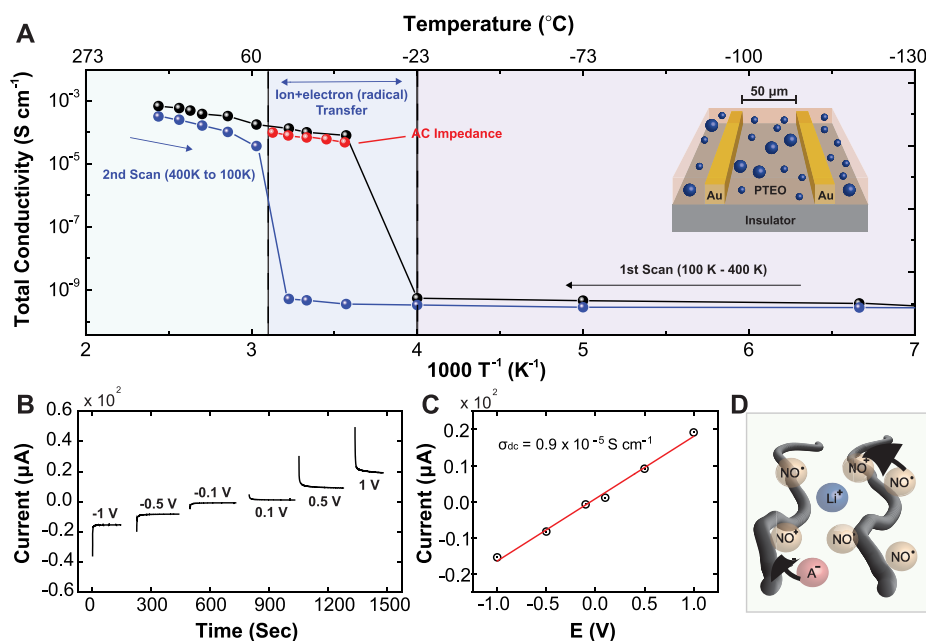
Figure 2. (A) Electrical conductivity as a function of temperature for PTEO in the channel length of 50 μm (the insets show the device architecture and the schematic illustration of charge transfer between the radical pendant groups for electronic conductors.). Two dominant transition points at −10 and 80 °C represent (1) an increase in the electrical conductivity of PTEO above T_g at around −10 °C and (2) a slight decrease in the electrical conductivity because of the disappearance of radical species around 80 °C. Radical density characterization as a function of temperature with (B) solution EPR spectra and (C) attenuated total reflection-Fourier transform infrared (ATR-FTIR) spectra in regard to the temperature. (D) Radical density calculated from the normalized peak at 1468 cm^{-1} (N−O$^{\bullet}$) by ATP-FTIR and the normalized intensity of EPR as a function of temperature.

which highlighted the import of maintaining a high open-shell radical density. To achieve this, we synthesized PTEO using a ring-opening polymerization (ROP) methodology with a lower initiator concentration to generate PTEO with a number-average molecular weight of 1.3 kg mol^{-1}. (Figure S2) Light absorption and electron paramagnetic resonance (EPR) spectroscopy data demonstrate that the synthesized material had an average of 0.98 nitroxide groups per repeat unit after polymerization (Figures 1C and S3A). Compared to the previous version of the PTEO,[1,31] we prepared the lower-molecular-weight PTEO with a lower glass transition temperature (T_g) of approximately −10 °C (Figure S3B), maintaining high radical density compared to that of the 4-hydroxy TEMPO (Figure S4). In general, as the T_g of the polymer is lowered, a polymer with a greater relaxation mode at room temperature can be obtained; therefore, the potential of achieving higher charge transport values at ambient conditions can be increased by lowering the T_g of the polymer.[38]

The coupling between ionic and electronic species is critical for solid-state electronics, batteries, and energy applications, and it is highly correlated to the chain dynamics of the polymer that has a disordered morphology. To test the effect of chemical doping of lithium ions on the chain dynamics of PTEO, the thermal characteristics of mixed PTEO−LiTFSI were measured (Figure S3B), and increasing amounts of lithium ions (LiTFSI) in the radical polymer resulted in increasing values of the glass transition temperature. This behavior has been observed beforehand in polyether-based (e.g., polyethylene oxide, PEO) systems, and it is ascribed to the formation of interactions between ionic species occurring

from the lithium salts and ether linkages in the polymer backbone owing to the physicochemical cross-linking.[39,40] In the context of this work, it suggests that there is a lowering of the chain mobility of the PTEO segments with increasing lithium salt concentrations. In addition, the amount of radical species observed using UV−vis and EPR spectroscopy decreased with the addition of LiTFSI (i.e., the +NO/NO$^{\bullet}$ ratio from N−O$^{\bullet}$ to $^{+}$N═O decreased to 18% with 10 wt % loading of LiTFSI) (Table S1).[29]

To characterize the details of the redox reaction between the PTEO and LiTFSI, we used X-ray photoelectron spectroscopy (XPS), where the nitrogen 1s (N$_{1s}$) peak demonstrates three separate chemical states of nitrogen in polymer or salts (Figure 1D). Each peak reveals the distinct chemical functionalities (N−O$^{\bullet}$, $^{+}$N═O, and N−OH) on the pendant groups of PTEO. The signal associated with the N−O$^{\bullet}$ functionality appears at 399.3 eV, which corresponds to the starting materials. It should be noted that the N^{-} peak from the TFSI appears at a similar location of N−O$^{\bullet}$ functionality (399.1 eV). Hence, in mixed formulations, the N−O$^{\bullet}$ functionality from PTEO and the N^{-} from TFSI^{-} overlap with one another. The peak at 397.9 eV is assigned to the N−OH, and the peak at the higher BE at 401.8 eV is correlated to $^{+}$N═O. In general, an increase in the oxidation state affects the binding energies of the oxidized groups to be higher. Utilizing XPS, the amounts of the cation analogue (PTEO^{+}) were quantified by both the presence of ionic species ($^{+}$N═O) on the polymer backbone and the LiTFSI ratio of salts, indicating that the radical active units are oxidized for the formation of $^{+}$N═O (Figure 1D). The intramolecular doping induces the pendant groups (N−

Figure 3. (A) Total conductivity as a function of temperature for PTEO−LiTFSI in the channel length of 50 μm. (B) Current vs time curves at various applied DC potentials. (C) Corresponding Ohm's law plot of steady-state current vs DC potential. Ohm's law was used to analyze the experimental data (open circle), and the DC conductivity was established as 0.9×10^{-5} S cm^{-1}. (D) Schematic illustration of charge transfer of ionic−electronic coupling for conductors.

O$^\bullet$) to be oxidized to ($^+$N=O) as the Li$^+$ cations are susceptible to being reduced to the charge-neutral state (Figure S5); this is confirmed by the acquisition of a similar XPS spectrum of the parent 4-hydroxy TEMPO−LiTFSI composite (Figure S6). Notably, the pendant groups (N−O$^\bullet$) can be converted to inactive sites (N−OH) due to the protonation, and this hinders the charge transfer as the N−OH sites can no longer participate in the redox reactions (Figure S7). This protonation might be due to the small amount of residual water in LiTFSI. In addition to confirming distinct nitrogen species analyzed in the N 1s peak, XPS spectroscopy also reveals the existence of the balancing ions in PTEO/LiTFSI [i.e., 55.7 eV for the lithium 1s (Li$_{1s}$) peak functionality (Figure 1E)]. However, a peak shift of Li$_{1s}$ is not clearly characterized due to the low signal-to-noise ratio and the sensitivity factor in PTEO−LiTFSI thin film. Together the UV−vis spectroscopy, EPR spectroscopy, and XPS analysis indicate the specific chemical formation of the PTEO radical polymer with the addition of LiTFSI under the optimized conditions.

We first monitored the solid-state electrical conductivity of a pristine (i.e., not doped) PTEO radical polymer in a channel with a length of 50 μm, and we analyzed the transition from the low charge transport to high charge transport regime in a temperature range of 100−400 K. This three orders of magnitude enhancement in electrical conductivity arises as the PTEO transitions from the glassy state to the molten state. For the evaluation of charge transport, the devices were relocated into the probe station at a temperature of 100 K under vacuum. Above the T_g of PTEO, the thin film displays a thermally activated charge transport regime, showing an activation energy of 133 kJ mol^{-1} that follows Arrhenian behavior (Figure 2A). This is due to the fact that there is increased molecular motion within the liquidlike materials at these elevated temperatures (below the degradation temper-

ature, Figure S8); thus, there is an increased likelihood of the radical−radical interaction.

The existence of a radical pendant group is characterized using both EPR and ATR-FTIR spectroscopy as a function of temperature (Figure 2B−D). In the temperature range of −10 to 80 °C, the difference in the current magnitude from the first and third scans could differentiate the electrical conductivity of radical pendant groups with different radical density values. This study demonstrated that the major charger transfer site is localized on the nitroxide group. The main governing factor for the ability of charge transport is to control the interactions between the radical pendant groups. Furthermore, with an understanding of the polymer chain dynamics regarding temperature, the operating domain area was enhanced to compare with the previous result. This phenomenon is mainly because of the enhanced chain mobility of PTEO leading to the formation of percolation of radical sites that are in electronic communication in the channel for long range (i.e., for lengths > 50 μm) as a percolation regime. For the wider applications of high-electrical-conductivity radical polymer (PTEO), we demonstrate the electrical conductivity of $\sim10^{-6}$ S cm^{-1} to be sustained over a large length scale.

To elucidate the effect of ions on the charge-neutral radical polymer, we used lithium bis(trifluoromethanesulfonyl)imide (LiTFSI), which is frequently used salt as a Li-ion source in electrolytes for Li-ion batteries.[41] In Figure 3A, we monitored the total conductivity transition in the PTEO−LiTFSI thin film device from the insulating regime ($\sim10^{-9}$ S cm^{-1}) to the high-conducting regime in real time ($\sim10^{-4}$ S cm^{-1}) from both DC and AC impedance measurements (Figure S9). The ion-conducting dominant behavior was observed in the PTEO−LiTFSI composite as the Nyquist plot showed both a capacitive tail and a semicircle due to ion transfer. Conversely, the Nyquist impedance data become a single semicircle as indicative of the electronic conductivity of pristine PTEO. Changing the channel length of the device maintained the high
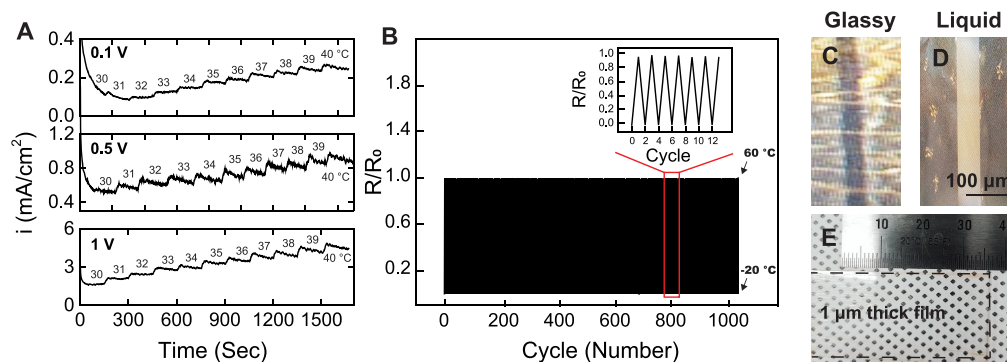
Figure 4. (A) Current density variation of PTEO−LiTFSI as a function of temperature in the range of 30−40 °C at different applied voltages. (B) PTEO−LiTFSI composite is quite sensitive to the temperature change in real time over 1000 cycles for solid-state electronics. The optical microscopy image of the radical polymer at different temperatures of −50 °C (C) and 50 °C. (D) Phase change of the radical polymer from the glassy to liquid state can be characterized. (E) Photograph of the PTEO−LiTFSI thin film to demonstrate the easy visibility behind PTEO−LiTFSI on a glass sample.

conductivity of the PTEO−LiTFSI blend in the range of 1−50 μm (Figure S10). Compared to that of the pristine PTEO, the variation of conductivity is much larger (i.e., a 5 order of magnitude jump in conductivity) as the addition of LiTFSI leads to increasing values of T_g. Upon the insertion of ions in the radical polymer, multiple factors affect the charge transfer, and these are the ionic−electronic coupling, ionic transport, and electronic transport.

To decouple these physical processes, we implemented DC polarization experiments.[33] Until a steady-state current was observed, the DC potential was applied to the blend device (Figure 3B). In Figure 3C, steady-state currents are plotted as a function of DC potentials. While ions were blocked at the gold electrodes, electronic charges were transported through the pathways continuously. Following Ohm's law, the electronic conductance of the material, σ_{dc}, is 0.95 × 10^{-5} S cm^{-1} at 40 °C. This is one order of magnitude higher than that of the pristine PTEO, indicating the intramolecular ion doping of LiTFSI for the radical polymer as the pedant groups are oxidized to oxoammonium cations (PTEO$^+$) in the active radical pendant groups in the polymer. Further addition of salts could affect the ion concentration; however, ionic cross-linking between ethylene oxide and lithium ions will occur simultaneously. As such, this interferes with segmental motions and thus ion and electronic transport cannot be effectively operated.[38] Critically, the existence of the PTEO$^+$ units upon the ion dopants influences the solid-state electrical conductivity of the PTEO organic radical polymer in a straightforward way (Figure 3D). As such, the highest electrical conductivity occurs at a mixture weight percentage of 10% ion (Figure S11). The average molar ratio of the PTEO monomeric units to lithium PTEO/LiTFSI was 15:1. We note that a channel containing a known electronically inactive polymer, PDMS-LiTFSI, was fabricated and tested to ensure that the total conductivity values ($\sigma \sim 9 \times 10^{-11}$ S cm^{-1}) in the micrometer channels were not due to the fabrication or processing conditions used in an organic electronic device (Figure S12).

To characterize the effect of ions on the chain dynamics of polymer, we implemented DSC (Figure S13). Notably, a melting transition occurs when LiTFSI is added to the PTEO matrix. The melting temperature (T_m) of pristine LiTFSI was ∼50 °C (Figure S14), which is quite above from the T_m of PTEO−LiTFSI, which was 118 °C. In the cooling cycle, which

takes the polymer into the glassy state, the PTEO−LiTFSI thin film shows a thermal transition at ∼70 °C. This behavior has been observed previously in polyether-based networks, and it is attributed to the organization of a coordination bond between lithium cations and oxygen atoms in macromolecular species.[39,42] Notably, there are some gaps between the transition point in the device and the T_m in DSC due to the difference in the physical properties of the polymer as thin films and in the bulk. Below T_m, the total conductivity of the PTEO−LiTFSI blend film decreased dramatically as the polymer mixture can be crystallized in the film lowering the ion transport (Figure 3D). It should be noted that chemical doping has made it possible to increase the electrical conductivity of PTEO but a tradeoff remains because the increase of dopants present in the PTEO lowers the chain mobility of the PTEO segments. This result indicates the fact that the physical property of a radical polymer is critical to transport the ion in the application of the device.

We analyzed the variation of the current density as a function of time with additional heating in the temperature range of 30−40 °C (Figure 4A). The current density increases with increasing temperature, and it is sensitive to voltage bias variations. Radical polymers maintained their total conductivity up to 1000 cycles by varying the temperature from the glassy state (−20 °C) to a viscous liquid state (60 °C) (Figure 4B). The change in the morphology was characterized by real-time optical microscopy (Figure 4C,D). While the glassy state is characterized below T_g, the radical polymer forms the liquidlike molten state for high conductivity. Together with this stability of radical under the temperature variation, we note that both undoped PTEO and PTEO−LiTFSI preserved the high electrical and ionic−electronic conductivity over multiple weeks upon exposure to ambient conditions; this result corresponds to the previous reports of the relative stability of the nitroxide radical when it is incorporated into the macromolecular.[1] Additionally, the completely amorphous nature of these materials is quite apparent in the samples, showing higher transparency with a 10 μm thick film (Figure 4E). The temperature-dependent characteristics and the nonconjugated nature of PTEO and the PTEO−ion blend could offer an exceptional opportunity in different fields such as organic electronics for solid-state electrodes, electrolytes, battery electrodes.

CONCLUSIONS

We have taken the first step in demonstrating the true potential of radical organic polymers as mixed ionic and electronic conductors. We elucidate the fundamental aspects of mixed conduction in nonconjugated organic radical polymers, establishing the charge conduction mechanism in solid-state electronic devices. The effective charge transport in the micrometer channel is realized by understanding the chain dynamics of radical polymer regimes, offering a clear design handle by which to engineer future generations of this type of open-shell polymer molecularly. These results illustrate the true potential in this new class blend of nonconjugated conducting polymers and ions for next-generation mixed ionic−electronic conductors.

ASSOCIATED CONTENT

ⓢ Supporting Information

The Supporting Information is available free of charge at https://pubs.acs.org/doi/10.1021/acs.macromol.0c00460.

> Experimental section for the PTEO synthesis and device characterization; chemical analysis of PTEO and the PTEO−LiTFSI composite; and AC impedance analysis (PDF)

AUTHOR INFORMATION

Corresponding Author

Yongho Joo − *Institute of Advanced Composite Materials, Korea Institute of Science and Technology (KIST), Wanju-gun, Jeonbuk 55324, Republic of Korea;* ⓞ orcid.org/0000-0002-1149-9105; Email: yjoo0727@kist.re.kr

Authors

Ilhwan Yu − *Institute of Advanced Composite Materials, Korea Institute of Science and Technology (KIST), Wanju-gun, Jeonbuk 55324, Republic of Korea*

Daeyoung Jeon − *Institute of Advanced Composite Materials, Korea Institute of Science and Technology (KIST), Wanju-gun, Jeonbuk 55324, Republic of Korea*

Bryan Boudouris − *Charles D. Davidson School of Chemical Engineering and Department of Chemistry, Purdue University, West Lafayette, Indiana 47906, United States;* ⓞ orcid.org/0000-0003-0428-631X

Complete contact information is available at:
https://pubs.acs.org/10.1021/acs.macromol.0c00460

Notes

The authors declare no competing financial interest.

ACKNOWLEDGMENTS

REFERENCES

(1) Joo, Y.; Agarkar, V.; Sung, S. H.; Savoie, B. M.; Boudouris, B. W. A nonconjugated radical polymer glass with high electrical conductivity. *Science* **2018**, *359*, 1391−1395.

(2) Zhang, Y.; Park, A. M.; McMillan, S. R.; Harmon, N. J.; Flatté, M. E.; Fuchs, G. D.; Ober, C. K. Charge Transport in Conjugated Polymers with Pendent Stable Radical Groups. *Chem. Mater.* **2018**, *30*, 4799−4807.

(3) Wang, S.; Easley, A. D.; Lutkenhaus, J. L. 100th Anniversary of Macromolecular Science Viewpoint: Fundamentals for the Future of Macromolecular Nitroxide Radicals. *ACS Macro Lett.* **2020**, *9*, 358−370.

(4) Song, Z.; Zhou, H. Towards sustainable and versatile energy storage devices: an overview of organic electrode materials. *Energy Environ. Sci.* **2013**, *6*, 2280−2301.

(5) Sato, K.; Ichinoi, R.; Mizukami, R.; Serikawa, T.; Sasaki, Y.; Lutkenhaus, J.; Nishide, H.; Oyaizu, K. Diffusion-cooperative model for charge transport by redox-active nonconjugated polymers. *J. Am. Chem. Soc.* **2018**, *140*, 1049−1056.

(6) Wang, S.; Li, F.; Easley, A. D.; Lutkenhaus, J. L. Real-time insight into the doping mechanism of redox-active organic radical polymers. *Nat. Mater.* **2019**, *18*, 69−75.

(7) Janoschka, T.; Hager, M. D.; Schubert, U. S. Powering up the future: radical polymers for battery applications. *Adv. Mater.* **2012**, *24*, 6397−6409.

(8) Rostro, L.; Galicia, L.; Boudouris, B. W. Suppressing the environmental dependence of the open-circuit voltage in inverted polymer solar cells through a radical polymer anodic modifier. *J. Polym. Sci., Part B: Polym. Phys.* **2015**, *53*, 311−316.

(9) Peng, Q.; Obolda, A.; Zhang, M.; Li, F. Organic light-emitting diodes using a neutral π radical as emitter: the emission from a doublet. *Angew. Chem., Int. Ed.* **2015**, *54*, 7091−7095.

(10) Neier, E.; Ugarte, R. A.; Rady, N.; Venkatesan, S.; Hudnall, T. W.; Zakhidov, A. Solution-processed organic light-emitting diodes with emission from a doublet exciton; using (2, 4, 6-trichlorophenyl) methyl as emitter. *Org. Electron.* **2017**, *44*, 126−131.

(11) Kemper, T. W.; Gennett, T.; Larsen, R. E. Molecular dynamics simulation study of solvent and state of charge effects on solid-phase structure and counterion binding in a nitroxide radical containing polymer energy storage material. *J. Phys. Chem. C* **2016**, *120*, 25639−25646.

(12) Bobela, D. C.; Hughes, B. K.; Braunecker, W. A.; Kemper, T. W.; Larsen, R. E.; Gennett, T. Close packing of nitroxide radicals in stable organic radical polymeric materials. *J. Phys. Chem. Lett.* **2015**, *6*, 1414−1419.

(13) Bässler, H.; Köhler, A. Charge Transport in Organic Semiconductors. In *Unimolecular and Supramolecular Electronics I*; Springer, 2011; pp 1−65.

(14) Chiang, C. K.; Fincher, C., Jr; Park, Y. W.; Heeger, A. J.; Shirakawa, H.; Louis, E. J.; Gau, S. C.; MacDiarmid, A. G. Electrical conductivity in doped polyacetylene. *Phys. Rev. Lett.* **1977**, *39*, No. 1098.

(15) MacDiarmid, A. G. "Synthetic metals": A novel role for organic polymers (Nobel lecture). *Angew. Chem., Int. Ed.* **2001**, *40*, 2581−2590.

(16) Shuai, Z.; Wang, L.; Song, C. *Theory of Charge Transport in Carbon Electronic Materials*; Springer Science & Business Media, 2012.

(17) Hutchison, G. R.; Ratner, M. A.; Marks, T. J. Hopping transport in conductive heterocyclic oligomers: reorganization energies and substituent effects. *J. Am. Chem. Soc.* **2005**, *127*, 2339−2350.

(18) Blauch, D. N.; Saveant, J. M. Dynamics of electron hopping in assemblies of redox centers. Percolation and diffusion. *J. Am. Chem. Soc.* **1992**, *114*, 3323−3332.

(19) Anson, F. C.; Blauch, D. N.; Saveant, J. M.; Shu, C. F. Ion association and electric field effects on electron hopping in redox polymers. Application to the tris (2, 2'-bipyridine) osmium (3+)/tris (2, 2'-bipyridine) osmium (2+) couple in Nafion. *J. Am. Chem. Soc.* **1991**, *113*, 1922−1932.

(20) Daum, P.; Lenhard, J.; Rolison, D.; Murray, R. W. Diffusional charge transport through ultrathin films of radiofrequency plasma polymerized vinylferrocene at low temperature. *J. Am. Chem. Soc.* **1980**, *102*, 4649−4653.

(21) Oyaizu, K.; Ando, Y.; Konishi, H.; Nishide, H. Nernstian adsorbate-like bulk layer of organic radical polymers for high-density charge storage purposes. *J. Am. Chem. Soc.* **2008**, *130*, 14459−14461.

(22) Janoschka, T.; Teichler, A.; Krieg, A.; Hager, M. D.; Schubert, U. S. Polymerization of free secondary amine bearing monomers by RAFT polymerization and other controlled radical techniques. *J. Polym. Sci., Part A: Polym. Chem.* **2012**, *50*, 1394−1407.

(23) Suga, T.; Pu, Y.-J.; Kasatori, S.; Nishide, H. Cathode-and anode-active poly (nitroxylstyrene) s for rechargeable batteries: p-and n-type redox switching via substituent effects. *Macromolecules* **2007**, *40*, 3167−3173.

(24) Nishide, H. Organic radical battery. *Electrochem. Soc. Interface* **2005**, *14*, 32−38.

(25) Tomlinson, E. P.; Hay, M. E.; Boudouris, B. W. Radical polymers and their application to organic electronic devices. *Macromolecules* **2014**, *47*, 6145−6158.

(26) Tokue, H.; Murata, T.; Agatsuma, H.; Nishide, H.; Oyaizu, K. Charge−Discharge with Rocking-Chair-Type Li+ Migration Characteristics in a Zwitterionic Radical Copolymer Composed of TEMPO and Trifluoromethanesulfonylimide with Carbonate Electrolytes for a High-Rate Li-Ion Battery. *Macromolecules* **2017**, *50*, 1950−1958.

(27) Suga, T.; Pu, Y.-J.; Oyaizu, K.; Nishide, H. Electron-transfer kinetics of nitroxide radicals as an electrode-active material. *Bull. Chem. Soc. Jpn.* **2004**, *77*, 2203−2204.

(28) Nishide, H.; Iwasa, S.; Pu, Y.-J.; Suga, T.; Nakahara, K.; Satoh, M. Organic radical battery: nitroxide polymers as a cathode-active material. *Electrochim. Acta* **2004**, *50*, 827−831.

(29) Rostro, L.; Wong, S. H.; Boudouris, B. W. Solid state electrical conductivity of radical polymers as a function of pendant group oxidation state. *Macromolecules* **2014**, *47*, 3713−3719.

(30) Rostro, L.; Baradwaj, A. G.; Boudouris, B. W. Controlled radical polymerization and quantification of solid state electrical conductivities of macromolecules bearing pendant stable radical groups. *ACS Appl. Mater. Interfaces* **2013**, *5*, 9896−9901.

(31) Lutkenhaus, J. A radical advance for conducting polymers. *Science* **2018**, *359*, 1334−1335.

(32) Gearba, I. R.; Nam, C.-Y.; Pindak, R.; Black, C. T. Thermal crosslinking of organic semiconducting polythiophene improves transverse hole conductivity. *Appl. Phys. Lett.* **2009**, *95*, No. 173307.

(33) Patel, S. N.; Javier, A. E.; Stone, G. M.; Mullin, S. A.; Balsara, N. P. Simultaneous conduction of electronic charge and lithium ions in block copolymers. *ACS Nano* **2012**, *6*, 1589−1600.

(34) Paulsen, B. D.; Tybrandt, K.; Stavrinidou, E.; Rivnay, J. Organic mixed ionic−electronic conductors. *Nat. Mater.* **2020**, *19*, 13−26.

(35) Winther-Jensen, B.; Winther-Jensen, O.; Forsyth, M.; MacFarlane, D. R. High rates of oxygen reduction over a vapor phase−polymerized PEDOT electrode. *Science* **2008**, *321*, 671−674.

(36) Savva, A.; Hallani, R.; Cendra, C.; Surgailis, J.; Hidalgo, T. C.; Wustoni, S.; Sheelamanthula, R.; Chen, X.; Kirkus, M.; Giovannitti, A.; Salleo, A.; McCulloch, I.; Inal, S. Balancing Ionic and Electronic Conduction for High-Performance Organic Electrochemical Transistors. *Adv. Funct. Mater.* **2020**, *30*, No. 1907657.

(37) Ji, H.-X.; Hu, J.-S.; Wan, L.-J.; Tang, Q.-X.; Hu, W.-P. Controllable crystalline structure of fullerene nanorods and transport properties of an individual nanorod. *J. Mater. Chem.* **2008**, *18*, 328−332.

(38) Zhao, Y.; Tao, R.; Fujinami, T. Enhancement of ionic conductivity of PEO-LiTFSI electrolyte upon incorporation of plasticizing lithium borate. *Electrochim. Acta* **2006**, *51*, 6451−6455.

(39) Le Nest, J.; Callens, S.; Gandini, A.; Armand, M. A new polymer network for ionic conduction. *Electrochim. Acta* **1992**, *37*, 1585−1588.

(40) Callens, S.; Le Nest, J.-F.; Gandini, A.; Armand, M. A novel solid polymer electrolyte: Synthesis and characterization. *Polym. Bull.* **1991**, *25*, 443−450.

(41) Kalhoff, J.; Bresser, D.; Bolloli, M.; Alloin, F.; Sanchez, J. Y.; Passerini, S. Enabling LiTFSI-based Electrolytes for Safer Lithium-Ion Batteries by Using Linear Fluorinated Carbonates as (Co) Solvent. *ChemSusChem* **2014**, *7*, 2939−2946.

(42) Chatani, Y.; Okamura, S. Crystal structure of poly (ethylene oxide)—sodium iodide complex. *Polymer* **1987**, *28*, 1815−1820.